Electrodeposition Kinetics in Li-S Batteries: Effects of Low Electrolyte/Sulfur Ratios and Deposition Surface Composition

Electrodeposition Kinetics in Li-S Batteries: Effects of Low Electrolyte/Sulfur Ratios and Deposition Surface Composition

Frank Y. Fan* **and Yet-Ming Chiang**,z**

Department of Materials Science and Engineering, Massachusetts Institute of Technology, Cambridge, Massachusetts 02139, USA

Lithium-sulfur batteries obtain most of their capacity from the electrodeposition of Li_2S. This is often a slow process, limiting the rate capability of Li-S batteries. In this work, the kinetics of Li_2S deposition from polysulfide solutions of 1–7 M S concentration onto carbon and two conductive oxides (indium tin oxide, ITO; and aluminum-doped zinc oxide, AZO) were characterized. Higher polysulfide concentrations were found to result in significantly slower electrodeposition, with island nucleation and growth rates up to 75% less than at low concentrations. Since Li-S batteries with low electrolyte/sulfur (E/S) ratios necessarily reach higher polysulfide concentrations during use, the present results explain why high polarization and low rate capability are observed under such conditions. Given that low E/S ratios are critical to reach high energy density, means to improve electrodeposition kinetics at high polysulfide concentrations are necessary. Towards this goal, coatings of ITO and AZO on carbon fiber current collectors were found to improve island growth rates at 5 M by up to ∼60%. Of the two oxides, AZO was found to be superior in reducing the electrodeposition overpotential. Its benefits were demonstrated for carbon fiber current collectors coated with AZO and for conductive suspensions incorporating carbon black and nanoparticle AZO.

Manuscript submitted December 27, 2016; revised manuscript received February 10, 2017. Published March 3, 2017. This was Paper 332 presented at the Phoenix, Arizona, Meeting of the Society, October 11–15, 2015.

Lithium-sulfur batteries are a promising technology for low-cost, high-density electrochemical energy storage beyond lithium-ion because of sulfur's high abundance, low cost, and high specific capacity (1670 mAh/g). The latter can enable, with a lithium metal negative electrode, a theoretical (active materials only) energy density of ∼2199 Wh/L or 2567 Wh/kg, with projected pack-level values of around 200–450 Wh/kg, which is significantly higher than that of current Li-ion batteries.[1–5] Energy density is highly dependent on the electrolyte content of the battery, however. In many published studies, the electrolyte/sulfur (E/S) ratio can be 10 mL/g or more.[6–8] At such a ratio, the large excess of electrolyte results in pack-level specific energy and energy density of less than ∼100 Wh/kg and 100 Wh/L, lower than that of present lithium-ion batteries, negating the theoretical advantage of the lithium-sulfur chemistry. By comparison, reducing the E/S ratio to 1 mL/g would enable up to ∼400 Wh/kg and 400 Wh/L.[2] Excess electrolyte also contributes additional cost to the battery. Unfortunately, several studies have also found that low electrolyte/sulfur ratio is correlated with poor rate capability and cycle life.[6,9]

Many of the challenges facing Li-S batteries arise from a charge/discharge mechanism that is fundamentally different from the intercalation reactions of conventional lithium-ion batteries. Instead, upon lithiation, sulfur first dissolves to form soluble lithium polysulfides Li_2S_x, $4 \leq x \leq 8$, which are then further reduced to insoluble Li_2S, which precipitates where the electronic charge transfer necessary for reduction can occur, typically on an electronically conducting carbon additive.[1,10–12] The polysulfides are soluble in concentrations of up to ∼8 mol S/L in ether solvents typically used in electrolytes. The electrolyte therefore undergoes significant changes in composition during each cycle, unlike batteries using intercalation cathodes. Therefore, the amount of electrolyte sets an upper bound on the concentration of polysulfides (Fig. 1). In a battery with an E/S ratio of 10 mL/g, the dissolution of all sulfur results in a polysulfide concentration of only 3.1 M, whereas a ratio of 1 mL/g would lead to a polysulfide concentration of 31 M, far in excess of the solubility limit. The electrolyte/sulfur ratio has significant effects on the composition and properties of the electrolyte, including ionic conductivity and exchange current density, as we have explored in a separate paper.[13]

Here, we investigate the effects of polysulfide concentration on the kinetics of the electrodeposition process. Although previous studies have shown decreased cycle life and rate capability as a result of low E/S ratio, this is the first one to quantify the effects of E/S ratio on the kinetics of the Li_2S electrodeposition process, which is responsible for the majority of the capacity in Li-S batteries.[6,9] We find that Li_2S deposition becomes remarkably sluggish at the high polysulfide concentrations found in Li-S batteries with low electrolyte content. The slower electrodeposition kinetics are correlated with significantly higher polarization and lower capacity and rate capability in Li-S cells with reduced electrolyte.

In addition, the influence of the conductive support material on electrodeposition kinetics has been investigated. Various materials have recently been evaluated as substitutes for carbon as conductive nucleation promoters, including metal oxides,[7,14–16] metal sulfides,[17,18] and conductive polymers.[19] Ionic compounds (that are also electronic conductors) in particular have been found to promote nucleation, which is attributed to their greater affinity for lithium sulfide. We compare the performance of bare carbon fiber electrodes to those

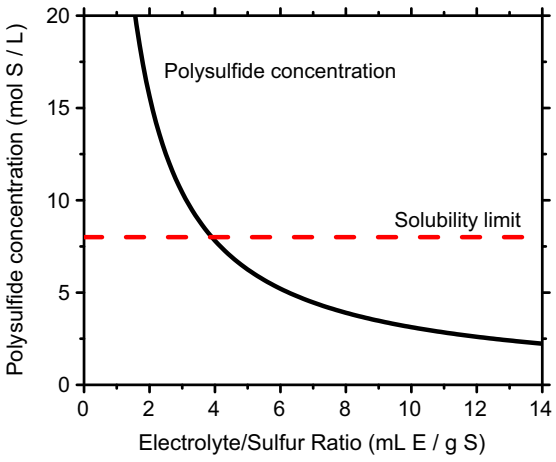

Figure 1. Polysulfide concentration in electrolyte if all sulfur is dissolved, vs electrolyte-sulfur ratio. Note that below a ratio of about 4 mL E/g S, the resulting polysulfide concentration exceeds the solubility limit. The concentration is calculated by dividing the molar mass of sulfur by the E/S ratio.

*Electrochemical Society Student Member.
**Electrochemical Society Member.
zE-mail: ychiang@mit.edu

coated with indium tin oxide (ITO) and aluminum-doped zinc oxide (AZO), and show that both oxides improve electrodeposition performance significantly. AZO, in particular, led to a greater improvement and is appealing because of the low cost of zinc. The addition of AZO to sulfur/carbon composite cathodes was shown to increase capacity and reduce polarization during galvanostatic discharge.

Experimental

All electrochemical testing was conducted using a Bio-Logic VMP 3 potentiostat. Preparation of electrolyte solutions and cell assembly were performed in an argon-filled glove box with oxygen and moisture contents below 1 ppm.

Potentiostatic testing of electrodeposition kinetics.—Polysulfide solution (Li_2S_6) was prepared by combining stoichiometric amounts of sulfur and Li_2S (Alfa Aesar) in a 1:1 by volume mixture of 1,2 dioxolane (DOL) and 1,3 dimethoxyethane (DME) (Sigma-Aldrich, used as received) and stirring for 24 h at 60°C. $LiNO_3$ (Sigma-Aldrich) and lithium bis(trifluoromethane) sulfonimide ("LiTFSI," BASF) were mixed into the polysulfide solution. Solid reagents were dried under vacuum overnight.

Testing was performed in 2-electrode Swagelok cells with a Li foil (Alfa Aesar) counter electrode. The Li was placed in electrolyte (0.5 M LiTFSI, 0.15 M $LiNO_3$, no polysulfide, in DOL/DME 1:1) for at least 1 h and then dried off prior to use. A porous polymer separator (Tonen Chemical Corporation, Tokyo, Japan) wetted with 6 ml of electrolyte was used to separate the two electrodes. The working electrode current collector was a Au-coated stainless steel rod with a 0.5 mm deep and 6.4 mm diameter well, into which a disk of carbon cloth (Avcarb 1071 HCB) was placed. ~22 mg of polysulfide solution was added to the carbon cloth. Cells were first held at 2.19 V for 2 h to reduce higher order polysulfides to Li_2S_4. They were then held at a potential of 2.05 V or 2.07 V to induce nucleation and growth of Li_2S, or an overpotential of 140 mV and 120 mV respectively. These potentials were chosen as they are close to the minimum observed at the beginning of the lower voltage plateau during a typical discharge. Potentiostatic intermittent titration technique (PITT) testing was performed in similar cells, using 5 mV potential steps and a current cutoff of C/400. Some PITT experiments used suspensions of carbon black (Ketjenblack EC-600JD) or AZO (~40 m^2/g, Nanoscale and Amorphous Materials, Inc.). Either 2.5 vol% carbon black or 25 vol% AZO (volume fractions chosen to maintain a consistent surface area) was suspended in 1 mol S/L polysulfide solution. Suspensions were first stirred manually, then sonicated for 30 min.

Cast electrode fabrication.—Sulfur powder (99.5%, Alfa Aesar), deionized water, carboxymethyl cellulose (CMC) binder, and Super-P carbon (Alfa Aesar) were mixed together for 30 min in a SPEX high-energy ball mill using polycarbonate milling media and container. The CMC was first dissolved in the water at a concentration of 16 mg/ml, and then mixed with the solid components to a target composition of 50% S, 44% Super-P, and 6% CMC by mass. For some electrodes, 10%, 50%, or 100% of the Super-P was replaced with an equivalent volume of AZO nanoparticles (20–40 nm, NanoAmor). The slurry was cast onto aluminum foil to a thickness of 0.25 mm, or a S loading of approximately 2 mg/cm^2. The slurry was allowed to dry under ambient conditions, and then further dried under vacuum. Swagelok cells were assembled using Li metal negative electrodes and carefully measured amounts of electrolyte to reach the target E/S ratios.

Indium tin oxide coated carbon fiber cloth.—Carbon fiber cloth was heated in air at 700°C for 10 min, then coated using a sol-gel process. The sol was prepared as described in Ref. 20 Tin (IV) acetate and indium (III) nitrate trihydrate (Alfa Aesar) were separately dissolved in ethylene glycol (Sigma Aldrich), the former at 80°C and the latter at ambient temperature. The two solutions were combined in a In^{3+}:Sn^{4+} molar ratio of 90:10 and stirred for 2 h at ambient temperature. The total concentration of cations was 0.5 M. Triethanolamine (Sigma-Aldrich) was added dropwise to a concentration of 0.25 M. The sol was diluted to a cation concentration of 0.2 M, coated on the carbon fiber cloth, then heat treated for 10 min at 400°C. These steps were repeated to increase the thickness, and the material was finally annealed in air for 1 h at 400°C. The target thickness was 150 nm.

Aluminum-doped zinc oxide coated carbon fiber cloth.—The same carbon fiber cloth was used as for the ITO coatings, without initial heat-treatment. Zinc oxide was prepared according to a previously published method.[21] Zinc(II) acetate dihydrate and aluminum nitrate nonahydrate (Alfa Aesar) were dissolved in ethanol to a Zn:Al molar ratio of 98:2 and a Zn^{2+} concentration of 0.4 M. Diethanolamine was added dropwise to reach a concentration of 0.4 M. This solution was stirred for 24 h and diluted to 0.1 M. The carbon cloth was coated with the liquid precursor solution, following which the cloth was dried at 300°C for 6 min. The coating and drying steps were repeated to increase the coating thickness. The films were then annealed at 400°C in air for 1 h. The target thickness was 150 nm. Resistivity for sol-gel AZO films is typically less than 10^{-3} Ωcm, corresponding to an area-specific resistance of less than 1.5×10^{-6} Ωcm^2 at this thickness.[22] Since typical current densities in our experiments are less than 0.1 mA cm^{-2}, we expect a negligible contribution to ohmic resistance from these films.

Scanning electron microscope characterization.—Samples were imaged in a Zeiss Merlin high-resolution SEM, with in-lens secondary electron detector and operating at 3 kV accelerating voltage.

Results and Discussion

Effects of E/S ratio on cell cycling.—Swagelok cells containing sulfur/carbon composite positive electrodes and lithium metal negative electrodes with E/S ratios of 7.9, 4.2 and 2.4 mL/g S were galvanostatically discharged at a rate of C/4 between the voltage limits of 2.6–1.7 V. As shown in Fig. 2, at the highest E/S ratio of 7.9 mL/g, which corresponds to the lowest dissolved sulfur concentration in the electrolyte of 3.9 M (assuming the sulfur is fully dissolved), the initial discharge capacity is 947 mAh/g. The discharge curve shows features typical of Li-S including a high voltage plateau and a regime of rapidly decreasing voltage corresponding respectively to the dissolution of sulfur and the reduction of higher order polysulfides, followed by a voltage "dip" centered at about 400 mAh/, followed by a voltage plateau corresponding to the co-existence of Li_2S_4 and solid Li_2S. As

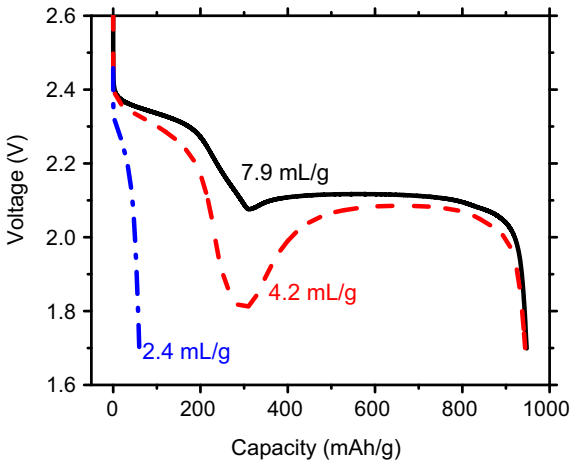

Figure 2. Galvanostatic (C/4) discharge curves for Li-S cells with sulfur-carbon composite cathodes at three different electrolyte/sulfur ratios. As the electrolyte/sulfur ratio decreases from 7.9 mL E/g S, the voltage drop at ~300 mAh/g, which corresponds to the onset of Li_2S nucleation and growth, increases dramatically in size before disappearing altogether. Electrolyte: DOL:DME 1:1, 0.5 M LiTFSI, 0.15 M $LiNO_3$.

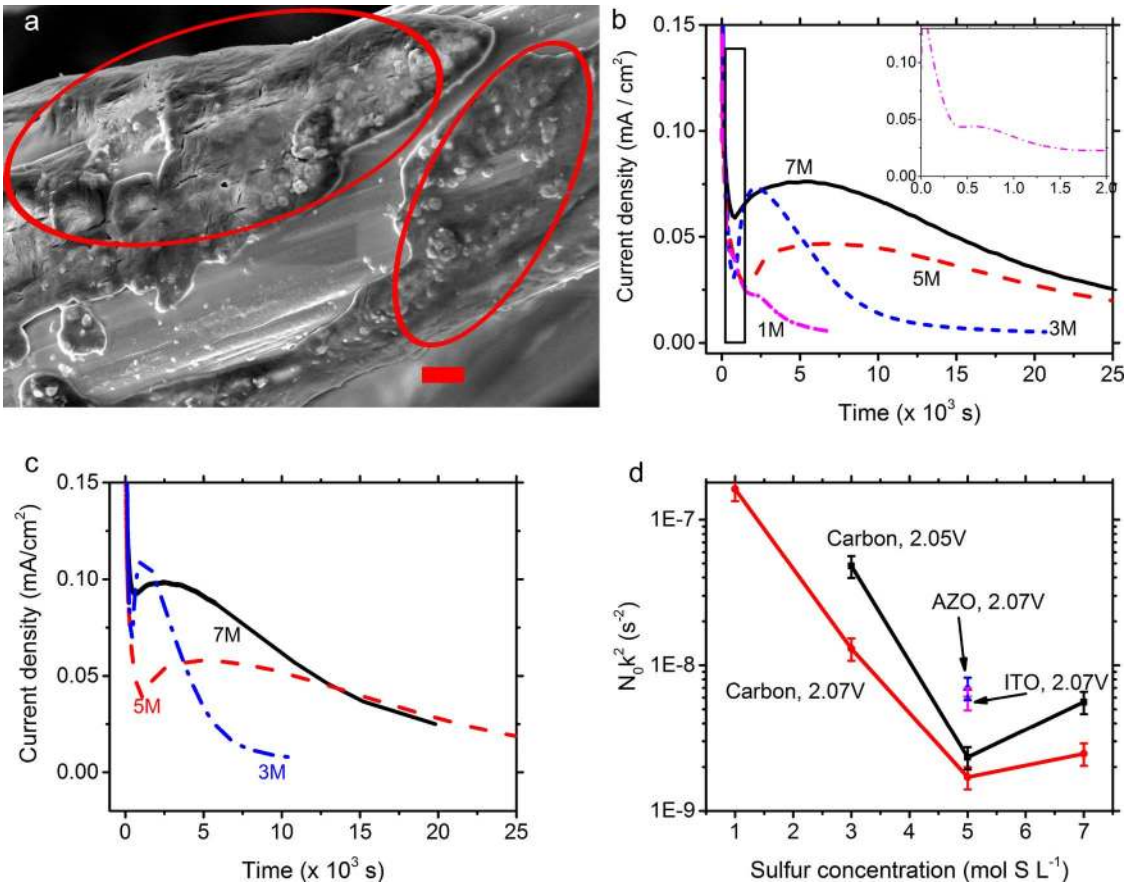

Figure 3. Effect of sulfur concentration on potentiostatic deposition. (a) Scanning electron microscope image of untreated carbon fiber after electrodeposition of Li_2S (2 h, 2.07 V, 3 mol S/L). Areas covered by sulfide are indicated in red. Scale bar: 1 μm (b) Current density vs time curves for electrodeposition on carbon at 2.07 V from polysulfide solutions of various concentrations. 1 M curve is enlarged in the inset. (c) Current density vs time curves for electrodeposition on carbon at 2.05 V (d) Values of N_0k^2 rate constant measured at various sulfur concentrations, on carbon at 2.05 V and 2.07 V, and on AZO and ITO at 2.07 V.

described in our previous work, the dip corresponds to the overpotential required for nucleation and initial growth of Li_2S.[12] The capacity is typical of a standard sulfur electrode, and the polarization on the plateau is 100 mV below the equilibrium voltage of 2.19 V.

At a lower E/S ratio of 4.2 mL/g, which corresponds to 7.4 M S, and is approximately the solubility limit of polysulfide at room temperature, the discharge capacity is nearly identical, but there is a significant increase in polarization. The increase in polarization is especially dramatic for the feature associated with nucleation and growth, where the minimum voltage now reaches 1.81 V as opposed to 2.08 V for E/S ratio of 7.9 mL/g S. Taken relative to the equilibrium voltage for the Li_2S plateau of 2.19 V, these voltage minima correspond to overpotentials of 380 mV and 110 mV for E/S of 4.2 and 7.0 mL/g S, respectively.[11,23–25] The nucleation and growth process clearly become much more sluggish as electrolyte volume decreases and maximum polysulfide concentration increases, as is further quantified below.

At a ratio of 2.4 mL/g (13 M S), the feature associated with nucleation and growth disappears altogether and the lower voltage plateau is not observed at all. The total capacity (<60 mAh/g) is much less than that which would be expected from the reduction of S to Li_2S_4 (~418 mAh/g), which typically occurs between ~2.5 V and 2.15 V. This may be because there was not enough electrolyte to dissolve the sulfur fully, given that the solubility is about 8 M S. Indeed, some studies have demonstrated that solid sulfur can exist throughout the discharge process without being fully dissolved.[10,26] This sulfur may limit access of the polysulfide to the carbon, limiting the effective surface area of the conductive carbon and increasing impedance due to sluggish reaction kinetics.

Electrodeposition experiments.—Potentiostatic electrodeposition experiments were performed at 2.07 V and 2.05 V vs Li/Li^+ (corresponding to the lower voltage plateau) on carbon cloth working electrodes using polysulfide solutions ranging from 1 M to 7 M (sulfur basis). The resulting current density vs time curves are shown in Figs. 3b and 3c, respectively.

The shape of these curves has been described in our previous work, in which we determined that electrodeposition occurs by a nucleation and 2D growth process on the carbon surface.[11,27] The current drops initially due to nonfaradaic double-layer charging and the reduction of remaining higher-order polysulfides. It then rises as nuclei of Li_2S are formed and grow larger, the current reaching a peak after which it decays due to impingement of nuclei and passivation of the surface by electronically insulating sulfide, which inhibits charge transfer. We determined that the current decay is not due to a diffusion limitation, as the decreasing portion of the current-time curve cannot be fitted using the Cottrell equation.[11,28,29] Under potentiostatic conditions (i.e. with a constant thermodynamic driving force) the process is well described by the Avrami equation (Equation 1), where Y is the fraction of total Li_2S that has been formed. In this particular system, the process can be modeled by a 2-dimensional island growth process with instantaneous nucleation. N_0 is the density of nuclei per unit area, and k is the lateral growth rate of islands.[30] The associated current vs time curve can thus be modeled using Equation 2, where J_m is the maximum current density and t_m is the time at which the maximum current occurs, and the current is proportional to the time derivative of Equation 1. Significantly, the nucleation density and growth rate (as a combined rate constant N_0k^2) can be determined using the time at which the

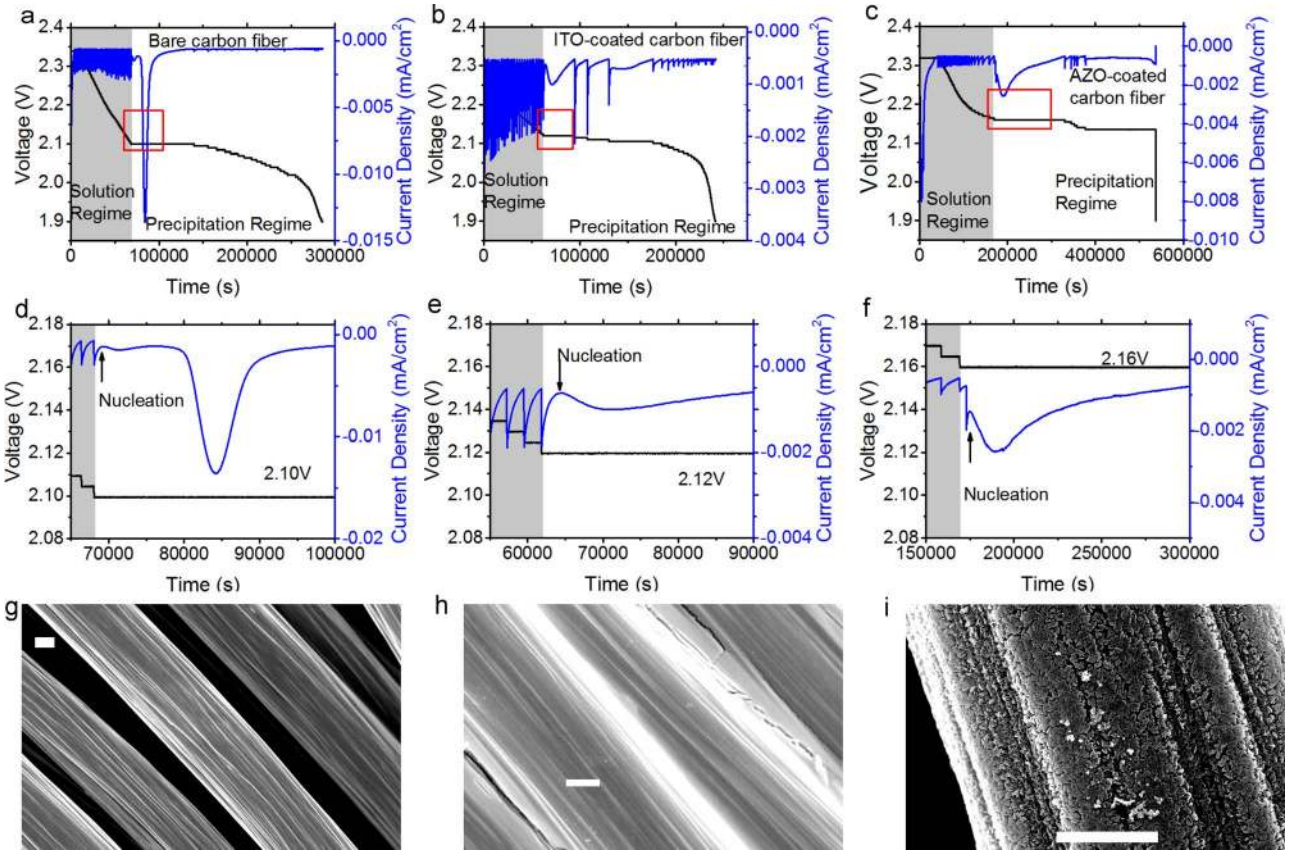

Figure 4. (a-f) Current and voltage vs time plots for PITT experiments for reduction of polysulfide solutions on bare carbon fiber (a,d), ITO-coated carbon (b,e), and AZO-coated carbon (c,f). d-f represent the portions in a-c that are highlighted in red. The large current peak in each plot represents the nucleation and growth of Li_2S. (g-i) Scanning electron microscope images of bare (g), ITO-coated (h), and AZO-coated (i) carbon fiber. All scale bars are 2 μm

current peak occurs, using Equation 3 (more nuclei and faster growth result in faster passivation of the surface, and an earlier onset of current decay). The value of t_m is independent of the surface area of the electrode, since both the spacing and growth rates of nuclei are fixed and the same amount of time passes before impingement occurs. The current minimum before the peak arises from the same phenomenon as the voltage minimum observed in galvanostatic discharge curves, i.e. the slow rate of transformation at the beginning of the phase change process. The background current resulting from double-layer capacitance and the reduction of higher-order polysulfides was fitted as the sum of two exponential decay functions (Fig. S1).

$$Y\ (t) = \ 1 - \exp\left(-\pi N_0 k^2 t^2\right) \qquad [1]$$

$$\frac{J\ (t)}{J_m} \propto \left(\frac{t}{t_m}\right) exp\left[-\frac{1}{2}\left(\frac{t^2 - t_m^2}{t_m^2}\right)\right] \qquad [2]$$

$$t_m = \left(2\pi N_0 k^2\right)^{-1/2} \qquad [3]$$

For electrodeposition on carbon at 2.07 V (Fig. 3a), considerable variation in N_0k^2 occurred as sulfur concentration was changed. For a 1 M solution, the peak corresponding to electrodeposition occurred almost immediately after the initial double-layer current, with a t_m value of only 990s. Increasing the concentration increases t_m to 3500s at 3 M, 9663s at 5 M and 8027s at 7 M. A similar pattern for t_m vs concentration was observed at 2.05 V (Fig. 3b). To estimate the error involved in this type of measurement, the 3 M (2.07 V) experiment was performed 13 times (Figure S2), and a standard deviation of 354s for t_m was obtained. We assumed a similar error of 10.1% of t_m would be present in measurements at other concentrations. The capacities obtained from Li_2S electrodeposition were approximately 270 mAh/g at 1 M, 250 mAh/g at 3 M, and 440 mAh/g at both 5 M and 7 M. This is considerably less than the theoretical capacity of 1250 mAh/g that would result from full conversion of polysulfides to Li_2S. That is, the current decay is due to passivation of the carbon surface and not depletion of sulfur. The N_0k^2 rate constants calculated from these values are plotted vs sulfur concentration in Fig. 3d. The value of N_0k^2 at 7 M is almost two orders of magnitude lower than that at 1 M. If both nucleation and growth are inhibited by the same factor, then N_0 and k at 7 M are only ~25% of their values at 1 M. Because of the very high concentration of polysulfide ions, ion pairing may inhibit redox reactions involving polysulfides. Reductions in reaction rate constants at high polysulfide concentrations have been observed previously.[13] Also, as expected, N_0k^2 was higher at 2.05 V than 2.07 V, i.e. at a greater overpotential. A small increase in N_0k^2 was observed from 5 M to 7 M. This may be because 7 M is near the solubility limit of polysulfides, and that some sulfide may have precipitated chemically (rather than electrochemically), forming nuclei for electrodeposition.

Effects of ITO and AZO surface coatings on electrodeposition kinetics.—The potentiostatic intermittent titration technique (PITT) was used to determine the critical overpotential needed to initiate nucleation of Li_2S on a given surface, with the results shown in Figs. 4–5. In Fig. 4, results are shown for carbon fiber cloth as the working electrode, either as-received (a,d,g) or coated with ITO (b,e,h) or AZO (c,f,i) via a sol-gel process, used with 1 M polysulfide solution. The uncoated carbon fiber cloth consists of relatively smooth fibers, as does the ITO-coated carbon. The AZO coating is rougher and consists of <100 nm nanoparticles. SEM images of all three are shown in Fig. 4. Lower-magnification images are provided in Fig. S3. ITO and AZO are conductive oxides which are commonly used as transparent electrodes in optoelectronic devices, and which have more

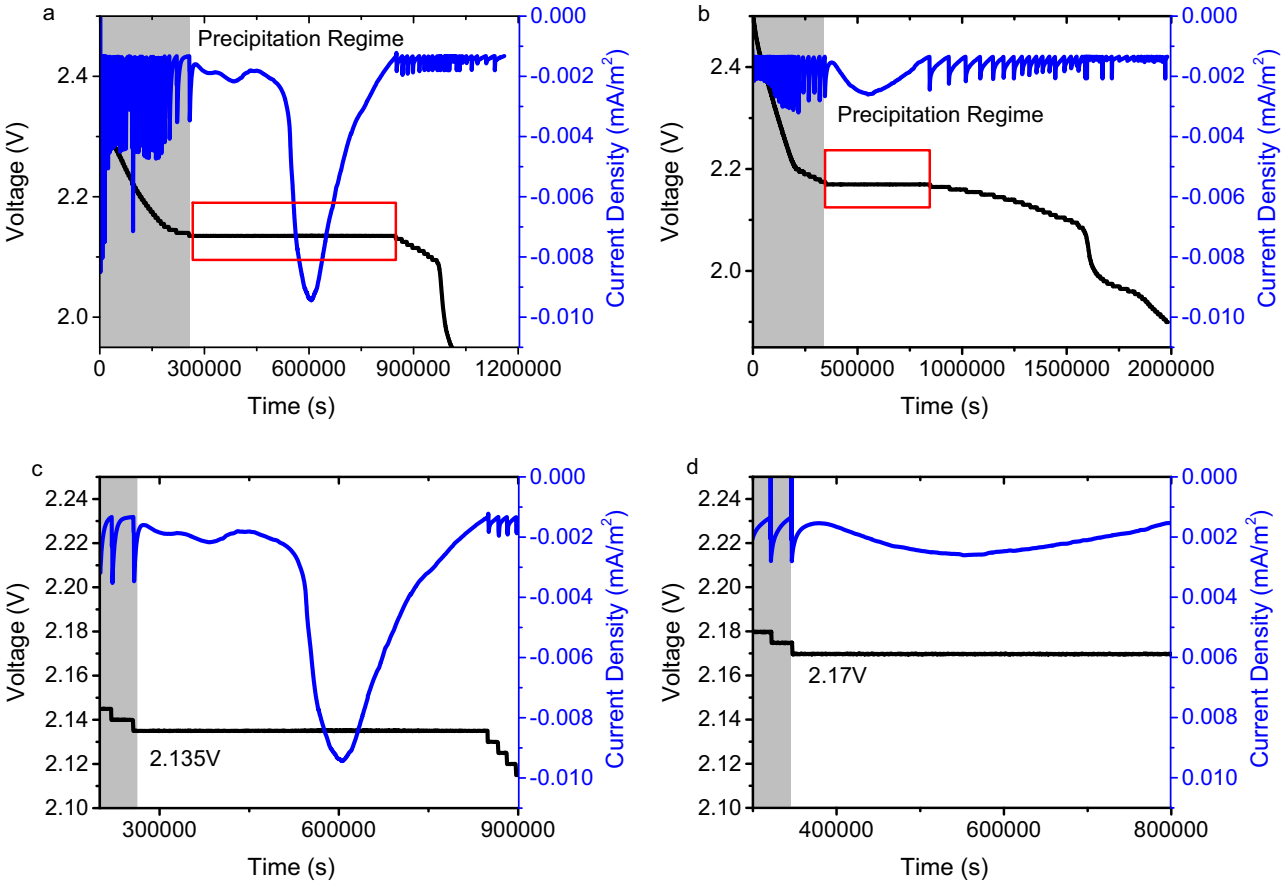

Figure 5. Current and voltage vs time plots for PITT experiments for reduction of 1 mol S/L polysulfide solution on suspended carbon black (a,c) and AZO nanoparticles (b,d).

recently been proposed as conductive additives for Li-S batteries.[7,16] Previous studies have found polar hosts, such as metal oxide, to bind more strongly to lithium sulfide than does non-polar carbon. Therefore, ITO and AZO would be expected to have lower energy barriers and smaller overpotentials for nucleation. From the open circuit potential, the working electrode potential was lowered in 5 mV steps, with the potential being stepped each time the current fell below a cutoff corresponding to C/400 rate. In the solution regime (between 2.3 V and 2.16 V, corresponding to the shaded regions in Fig. 4), current decreased monotonically during each step, which is expected from a process with no phase change, i.e. the reduction of soluble polysulfides to lower-order soluble polysulfides. The first potential step in which a current maximum indicating nucleation and growth appears corresponds to the minimum overpotential that can initiate nucleation, and the beginning of the precipitation regime. Carbon required the greatest overpotential (90 mV) followed by ITO (70 mV) and AZO (30 mV).

Based on these results alone, it is not clear whether the lower overpotential for the AZO-coated carbon is due to its higher surface area compared to the bare carbon fiber, or to the presence of AZO. Therefore, PITT experiments were also conducted on suspension-based polysulfide electrodes with identical surface areas of carbon black and AZO nanoparticles. The suspension electrode approach, first shown in Ref. 12, uses a continuously percolating network of conductive particles to create a "current collector" of high surface area and extending throughout the volume of the polysulfide solution. Using the same carbon and AZO surface area, and the same current cutoff of C/400, a lower overpotential was again observed for AZO (20 mV) than for carbon black (55 mV), as shown in Fig. 5. This comparison shows that it is the AZO that reduces the overpotential. Note that lower overpotentials were observed for both suspensions compared to their carbon fiber counterparts (uncoated and AZO coated). This is attributed to the fact that both nanoparticle suspensions have much greater surface area, by a factor of ~200, than the carbon cloth. Therefore, the actual current density per area of solid conductor at the PITT cutoff current density is also lower by about the same factor of ~200. This experiment confirms that using a conductive nanoparticle suspension instead of carbon fiber as the electrode increases the electrochemically active surface area and reduces polarization, a result we first showed in a previous paper.[12]

To quantify the effects of oxide coating on the reaction rate constant, N_0k^2, under electrolyte-lean conditions, potentiostatic electrodeposition experiments were then performed at 2.07 V using 5 M polysulfide solutions and the coated carbon fiber electrodes (Fig. 6a). Both coated electrodes yielded faster kinetics than the uncoated one, the increase in N_0k^2 being about a factor of 3.1 and 2.5 for AZO and ITO, respectively (Fig. 3d). In fact, the current minimum that is characteristic of a nucleation barrier disappeared entirely for the AZO-coated electrode. We attribute the faster kinetics of electrodeposition on AZO compared to ITO, as well as the lower overpotential required for nucleation, to stronger binding between AZO and Li_2S.

Further investigating the effects of AZO as a nucleation promoter, experiments were conducted under galvanostatic discharge conditions. Cathodes were prepared which were similar to the S/C composite cathodes tested above, but with 10%, 50%, or 100% of the Super-P carbon being replaced with the same volume of AZO nanoparticles. Cells containing such cathodes were discharged under identical conditions to those in Fig. 2, and at the same 4.2 mL/g E/S ratio (cf. middle curve in Fig. 2). The resulting discharge curves, along with the one for the original cathode without AZO, are shown in Figure 6b. Nucleation overpotentials of 230 mV and 155 mV were respectively observed for the 10% and 50% samples, compared to 380 mV

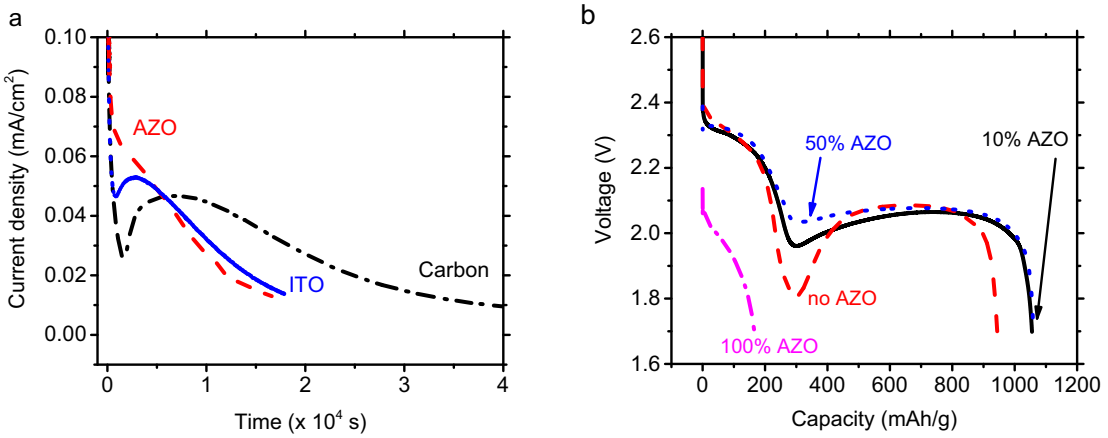

Figure 6. (a) Potentiostatic (2.07 V) current density vs time data for electrodeposition of Li2S from 5 M polysulfide solution onto carbon and AZO and ITO coated carbon. (b) Galvanostatic discharge curves for Li-S cells with a S/C cathode and a S/C/AZO cathode (solid, black). The latter exhibits a significantly lower nucleation overpotential, observed at ∼300 mAh/g capacity, as well as higher total capacity.

in the original discharge curve. Moreover, specific capacity increased from to 945 mAh/g to 1055 mAh/g and 1060 mAh/g respectively. The lower initial overpotential for the AZO/C composite cathodes likely causes Li_2S to deposit preferentially on isolated AZO particles while reducing the number of nuclei forming on carbon, resulting in electrodeposition which is dominated by growth from AZO sites rather than nucleation of Li_2S islands on carbon. A reduced nuclei density has been shown in our previous work to be associated with delayed passivation and fewer, larger Li_2S particles and more Li_2S deposited on a given electrode surface area.[11] Figure 6b shows that replacement of all carbon with AZO, on the other hand, leads to a very large overpotential (over 250 mV greater than carbon-containing electrodes) during the sulfur dissolution step. Moreover, capacity decreased to less than 200 mAh/g, even less than the capacity expected from sulfur dissolution. We believe that excessively strong binding between substrate and polysulfide may have negative effects in this instance, namely the difficulty of desorbing polysulfide reaction products from the surface during the S_8 dissolution step. Thus a hybrid cathode containing both carbon and oxide can offer lower polarization than one containing carbon or oxide alone.

Cycle life data for both S/C and S/C/AZO composite cathodes is shown in Fig. S4. A slight improvement in cycle life was observed for AZO-containing electrodes, although cycle life for both types of electrode was quite poor, with most of the initial capacity lost within 20 cycles. However, these electrodes were not designed for maximizing cycle life, but only to demonstrate the effects of different surfaces on polarization. Hence, standard methods for improving cycle life via polysulfide encapsulation were not used, and cells suffered from degradation via typical mechanisms such as polysulfide shuttling.

Conclusions

The kinetics of lithium sulfide electrodeposition on carbon and metal oxide surfaces from polysulfide solutions of various concentrations were measured using chronoamperometric tests and a variety of electrode configurations. Electrodeposition was found to be significantly slower at high polysulfide concentrations for a given deposition substrate. Because electrolyte/sulfur ratio affects the polysulfide concentration reached in the electrolyte during use, we believe that the dependence of precipitation kinetics on dissolved sulfur concentration is responsible for sluggish Li_2S electrodeposition during cycling of Li-S batteries. Indeed, we observed significantly larger nucleation barriers in our model Li-S cells when cycling them under electrolyte-lean conditions. Promoting the electrodeposition of Li_2S is therefore an important consideration when designing electrolyte-lean Li-S batteries. ITO and AZO surfaces were found to improve nucleation and growth performance at high polysulfide concentrations; AZO may be preferred due to its lower cost. The addition of AZO to sulfur/carbon composite cathodes was found to reduce polarization and increase capacity under galvanostatic cycling conditions. These improvements were observed both for stationary carbon fiber current collectors and for conductive suspensions in which a percolating network of carbon forms a spatially-extended current collector.

Acknowledgments

This work was supported as part of the Joint Center for Energy Storage Research, an Energy Innovation Hub funded by the U. S. Department of Energy, Office of Science, Basic Energy Sciences.

References

1. P. G. Bruce, S. A. Freunberger, L. J. Hardwick, and J.-M. Tarascon, *Nat. Mater.*, **11**, 19 (2012).
2. D. Eroglu, K. R. Zavadil, and K. G. Gallagher, *J. Electrochem. Soc.*, **162**, A982 (2015).
3. M. Barghamadi, A. Kapoor, and C. Wen, *J. Electrochem. Soc.*, **160**, A1256 (2013).
4. X. Ji and L. F. Nazar, *J. Mater. Chem.*, **20**, 9821 (2010).
5. Y. Yang, G. Zheng, and Y. Cui, *Energy Environ. Sci.*, **6**, 1552 (2013).
6. J. Zheng et al., *J. Electrochem. Soc.*, **160**, A2288 (2013).
7. H. Yao et al., *Nat. Commun.*, **5**, 3943 (2014).
8. L. Qie and A. Manthiram, *Adv. Mater.*, **27**, 1694 (2015).
9. S. Zhang, *Energies*, **5**, 5190 (2012).
10. M. Cuisinier et al., *J. Phys. Chem. Lett.*, **4**, 3227 (2013).
11. F. Y. Fan, W. C. Carter, and Y.-M. Chiang, *Adv. Mater.*, **27**, 5203 (2015).
12. F. Y. Fan et al., *Nano Lett.*, **14**, 2210 (2014).
13. F. Y. Fan et al., *J. Electrochem. Soc.* (2016).
14. Q. Pang, D. Kundu, M. Cuisinier, and L. F. Nazar, *Nat. Commun.*, **5**, 4759 (2014).
15. X. Tao et al., *Nano Lett.*, **14**, 5288 (2014).
16. X. Gu et al., *Electrochim. Acta*, **196**, 369 (2016).
17. Z. Yuan et al., *Nano Lett.*, **16**, 519 (2016).
18. Q. Pang, D. Kundu, and L. F. Nazar, *Mater. Horiz.*, **3**, 130 (2016).
19. G. Zheng et al., *Nano Lett.*, **13**, 1265 (2013).
20. S.-S. Kim, S.-Y. Choi, C.-G. Park, and H.-W. Jin, *Thin Solid Films*, **347**, 155 (1999).
21. M. Wang et al., *Mater. Lett.*, **61**, 1118 (2007).
22. W. Tang and D. C. Cameron, *Thin Solid Films*, **238**, 83 (1994).
23. D. N. Fronczek and W. G. Bessler, *J. Power Sources*, **244**, 183 (2013).
24. M. Marinescu, T. Zhang, and G. J. Offer, *Phys. Chem. Chem. Phys.* (2015).
25. D. Marmorstein et al., *J. Power Sources*, **89**, 219 (2000).
26. R. Elazari et al., *J. Electrochem. Soc.*, **157**, A1131 (2010).
27. A. Bewick, M. Fleischmann, and H. R. Thirsk, *Trans. Faraday Soc.*, **58**, 2200 (1962).
28. G. Gunawardena, G. Hills, I. Montenegro, and B. Scharifker, *J. Electroanal. Chem. Interfacial Electrochem.*, **138**, 225 (1982).
29. M. Jafarian, M. G. Mahjani, F. Gobal, and I. Danaee, *J. Electroanal. Chem.*, **588**, 190 (2006).
30. M. Avrami, *J. Chem. Phys.*, **7**, 1103 (1939).